Modelling DNA replication fork stability and collapse using chromatin fiber analysis and the R-ODD-BLOBS program

AUTHORS:
Kerenza Cheng[1], Kazeera Aliar[2], Roozbeh Manshaei[3], Ali Mazalek[1,3], Sarah A Sabatinos[1,2,*]

AFFILIATIONS

1 – Molecular Science Graduate Program, Yeates School of Graduate and Postdoctoral Studies, Toronto Metropolitan University, Toronto ON M5B 2K3

2 – Department of Chemistry and Biology, Toronto Metropolitan University, Toronto ON M5B 2K3

3 – SynLab, The Creative School, Toronto Metropolitan University, Toronto ON M5B 2K3

* – correspondence: ssabatinos@torontomu.ca, www.SabatinosLab.net

KEYWORDS: DNA replication fork, *Schizoasaccharomyces pombe,* hydroxyurea (HU) arrest, DNA recombination

RUNNING TITLE: Fork stability and collapse analysis

ABBREVIATIONS: Double strand break (DSB), bromodeoxyuridine (BrdU), *Schizosaccharomyces pombe* (*S. pombe*), homologous recombination (HR), double strand DNA (dsDNA), single stranded DNA (ssDNA), One Dimensional Data – Boolean Logic Operations Binning System (ODD-BLOBS),

ABSTRACT

We describe the anatomy of replication forks by comparing the lengths of synthesized BrdU-labelled DNA in wild-type, *mrc1Δ* and *cds1Δ Schizoasaccharomyces pombe*. We correlated Rad51 and Cdc45 proteins relative to their positions on the fork, replicated tract, or unreplicated regions. We did this using chromatin spread pixel intensity data that was analyzed using our program: R-ODD-BLOBS. Graphs on the lengths of BrdU tract, and proteins, as well as the percentage of Rad51 and Cdc45 colocalization, were created by the program. These results were compared to the literature. The BrdU lengths detected matched current literature; cds1Δ was the longest at 8.6 px, wild-type was 7.5 px, and mrc1Δ was the shortest at 5.1 px. When colocalization of rad 51 around the fork was explored, we found that mrc1Δ uniquely had 22% more colocalization than wt at the unreplicated region of a fork. This suggests that HR was potentially detected at the forks of mrc1Δ. In this study, we summarize the usefulness of R-ODD-BLOBS in aiding in analyzing chromatin spread data which provides data on the lengths and protein colocalization and starts to paint a picture of the anatomy of a fork.

SIGNIFICANCE STATEMENT

- The dynamics of a replication fork are important to maintaining genome stability, however, current methods create an average bulk data that can conceal the heterogeneity of forks.
- This pipeline involving chromatin spread fiber, and data analysis using R-ODD-BLOBS establishes a single-molecule approach to a dynamic problem that can determine patterns like differences in synthesized DNA between conditions, and determine colocalization of proteins at different regions on chromatin, while systematically determining parameters
- This pipeline shows and quantifies patterns found in chromatin spread fibers, while maintaining the option to average out data or individually look at them

INTRODUCTION

High-fidelity DNA replication and active response to replication stress are critical to genome stability and cancer avoidance (Hyrien, 2000; Lambert *et al.*, 2007). The replication fork complex consists of two linked activities that ensure DNA replication is efficient, speedy and faithful (Noguchi *et al.*, 2004; Nedelcheva *et al.*, 2005; Errico *et al.*, 2009; O'Donnell and Li, 2016). First, the Cdc45-MCM-GINS (CMG) helicase complex unwinds the DNA template ahead to promote high-speed copying of the genome (Walter and Newport, 2000; Pacek and Walter). Second, DNA polymerases on the leading (polymerase ε) and lagging (polymerases Δ and α) strands create two copies of DNA to be split between daughter cells at division (Tanaka *et al.*, 2009; Daigaku *et al.*, 2015; Yurieva and O'Donnell, 2016). In addition, claspin/mrc1Δ1 protein is a part of the Fork Protection Complex that directly connects pol to the helicase complex (e.g. (Lou *et al.*, 2008; Nitani *et al.*, 2008)). Claspin/mrc1Δ1 also influences replication processivity and independently activates cds1Δ1 for the replication checkpoint (Lee *et al.*, 2005; Szyjka *et al.*, 2005; Nitani *et al.*, 2008; Ünsal-Kaçmaz *et al.* 2007; Alabert *et al.*, 2009; Kemp *et al.*, 2010). The replication checkpoint responds to a variety of naturally occurring and exogenous impediments that cause replication fork slowing and/or stalling (Calzada *et al.*, 2005). A drug with this mechanism is hydroxyurea (HU), which depletes dNTP pools and causes forks to slow and arrest (Snyder, 1984; Koç *et al.*, 2004; Sabatinos *et al.*, 2013a). In fission yeast also known as *Schizosaccharomyces pombe* (*S. pombe*), the protein cds1Δ1 promotes stable replication arrest in the presence of HU. The ribonucleotide reductase activity is "poisoned" and causes a decrease in dNTP levels (Sabatinos *et al.*, 2013b). The arrest prevents late origin firing which rescues the

remainder of the DNA replication programme (Sabatinos *et al.*, 2013a). In a cds1Δ1Δ mutant, cells continue to synthesize DNA in HU and acquire DNA damage. This leads to a lethal G2 arrest and can be seen as *S. pombe* cell elongation.

During DNA damage, there are two major pathways in which a cell can repair double-strand DNA breaks (DSB) damage. One method of DSB is homologous recombination (HR) which is often used when only one DNA end remains (Taylor *et al.*, 2015; Bonilla *et al.*, 2020). This pathway is initiated by the complex called mre11-rad50-nbs1 and with CtIP, recognizes the DSB and the protein Rad51 subsequently associates with single-stranded DNA (ssDNA) (Bonilla *et al.*, 2020). Rad51 is activated by its mediators, in *S.pombe* this is rad52 and others, and the Rad51 searches for homologous regions to serve as a template for repair (Benson *et al.*, 1998; Bonilla *et al.*, 2020).

Furthermore, our understanding of replisome dynamics during HU block primarily comes from molecular work where immune-precipitated enrichment is averaged across a population using sequencing, or isolation of proteins on nascent DNA (iPOND) (Feng *et al.*, 2006; Rozenzhak *et al.*, 2010; Sirbu *et al.*, 2011). These techniques show bulk protein movement and association with specific sequences. However, the average response across a population may obscure some events through “ensemble averaging” (Oijen, 2007; Stratmann and Oijen, 2014). Thus, the behavior of sub-populations with alternate phenotypes is lost (Cortez, 2015), making it impossible to understand the diversity and range of phenotypes that can allow us to further understand behaviors.

Other experiments using electron microscopy have also imaged DNA replication forks and detected increased ssDNA at individual forks during arrest and replicon components show association and structure, but in the absence of genome context and adjunct replicon members (Sogo *et al.*, 2002; Yurieva and O'Donnell, 2016).

We combine microscopy and molecular labeling to understand protein dynamics in the replication as further research into these associations would provide insight into replication dynamics, genetic diseases, and cancer but the compaction of DNA hinders this process. Thus, chromatin fiber analysis is an inexpensive and high-content method that retains proteins, enabling the direct detection of replication complexes on DNA with fluorescent tagging. The main hindrance of this technique is the large amount of DNA that is generated; this proves to be a challenge to analyze and model. A previous program called One Dimensional Data – Boolean Logic Operations Binning System (ODD-BLOBS) was developed as an analysis tool to systematically correlate DNA synthesis with protein location using chromatin fiber data. ODD-BLOBS measures tract lengths to determine replication processivity or instability. ODD-BLOBS has been re-implemented to be more robust and user-friendly in the programming language R (now R-ODD-BLOBS).

We use DNA-chromatin spread fibers to look at wildtype (wt), *mrc1*Δ and *cds1Δ S.pombe* mutants. A thymidine analogue bromodeoxyuridine (BrdU) was used to label newly synthesized DNA after a 30-minute block in HU had been performed, allowing the identification of potential replication fork zones and markers of DNA damage. Both

Cdc45 and Rad51 were tagged using immunofluorescence to determine potential changes to colocalization in response to HU. We show that the mean lengths obtained by R-ODD-BLOBS accurately reflect the condensed and filamentous nature of the DNA as well as proteins. We also show that the colocalization determined by R-ODD-BLOBS potentially can detect HR in *mrc1Δ* through Rad51 colocalization within the fork and further in the unreplicated regions. By standardizing chromatin fiber data analysis methods, we correlate protein position relative to synthesis in the visual anatomy of the replication fork. This establishes a single-molecule approach to a dynamic problem.

RESULTS

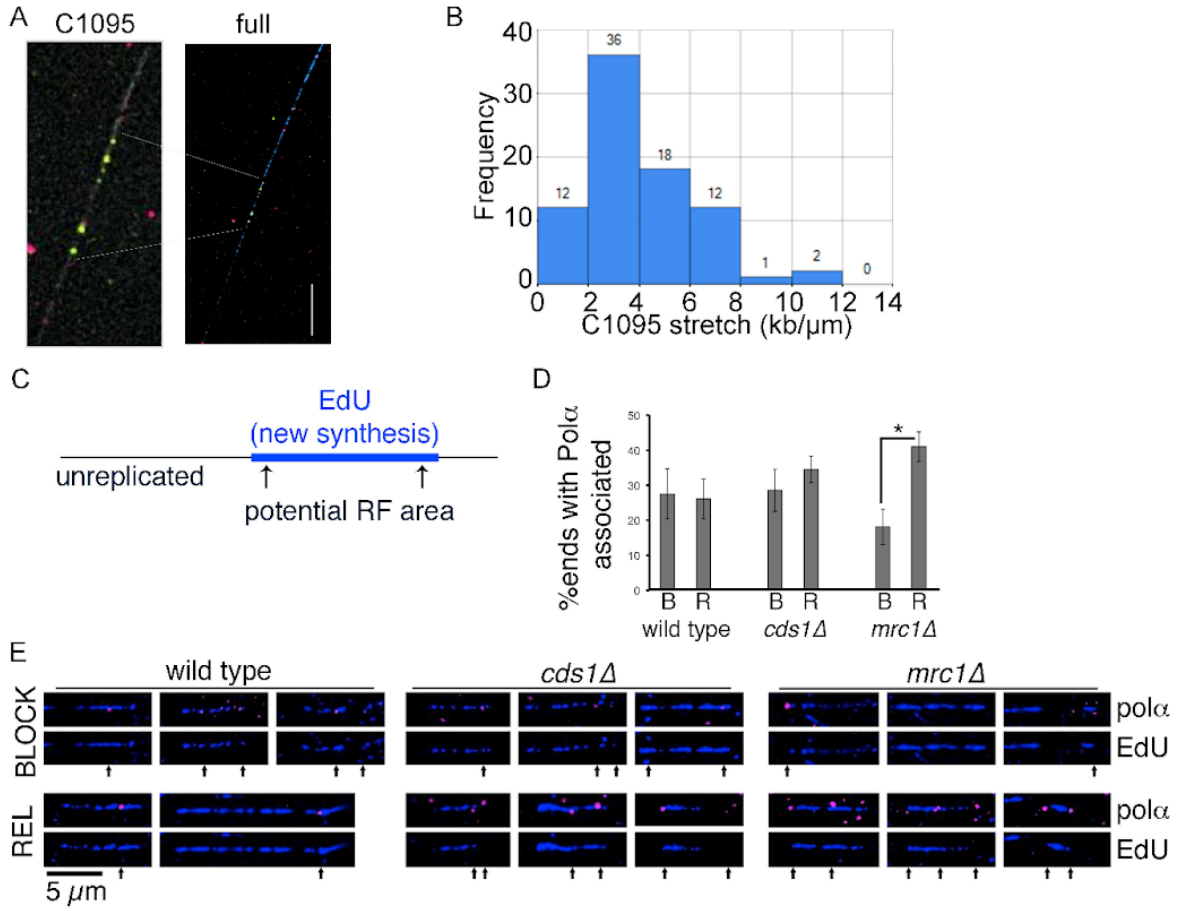

Figure 1 Data analysis of wt, cds1Δ and *mrc1Δ* on polα using ODD-BLOBS. Prior data were analyzed using ODD-BLOBS, this is an older version that uses VBA. This experiment visualizes newly synthesized tracts using EdU with primase (pola). (A) A fluorescent microscopy image of a chromatin spread fiber. The image on the right is the full image, and the image on the left enlarges a portion to highlight the fluorescence in-situ hybridization (FISH) cosmid probe that was hybridized to fibers at the c1095 region. (B) The frequency of C1095 distance as a histogram. The average stretch of fibers is approximately 3 kb/μm. (C) Scheme for analyzing replicated tracts on spread DNA fibers. Each replicated tract has an internal (replicated) zone and external unreplicated areas. We defined the ends of each synthesized tract as potential replication fork areas. Bi-directional replicons would have 2 forks, uni-directional replicons would only have 1 fork. (D) DNA polα (FLAG-Pol) was analyzed relative to EdU incorporation and tract-ends (potential replication fork areas). EdU ends with Polα are presented as the percent of total ends examined during block (labelled B) and release (labelled R), 95% CI. (E) Microscopy images of Polα (tagged in pink) at EdU tract-ends (tag in blue) during HU (BLOCK) and release (REL). Polα in potential replication fork areas are indicated by arrows under the image.

A previous version, called ODD-BLOBS analyzed another set of chromatin fiber data. This version uses Visual Basic for Applications (VBA) script. From the microscopy image shown in Fig 1A,F the intensity data is obtained for newly synthesized tracts from EdU and polα during HU block and release. The frequency of C1095 lengths was obtained, and lengths of 3 kb/μm occurred the most as seen in Fig 1B. A schematic of the logic of unreplicated regions, tracts, and forms is determined, as seen in Fig 1C, with ends of newly replicated areas labelled with a fluorescent nucleotide analogue (in Fig 1 this is EdU, and in the remaining figures this would be BrdU) are defined as potential fork end areas. The percentage of polα colocalization at the fork ends was compared during HU block and after its release. As seen in Fig 1D, end-associated Polα is similar in wild type and cds1Δ1Δ, during and after release but *mrc1Δ* tract ends show increased Pol after HU release. This high colocalization can also be seen in the microscopy images (Fig 1E), polα represented by the pink had an increased presence after release in *mrc1Δ*.

<u>Thresholding analysis using R-ODD-BLOBS</u>

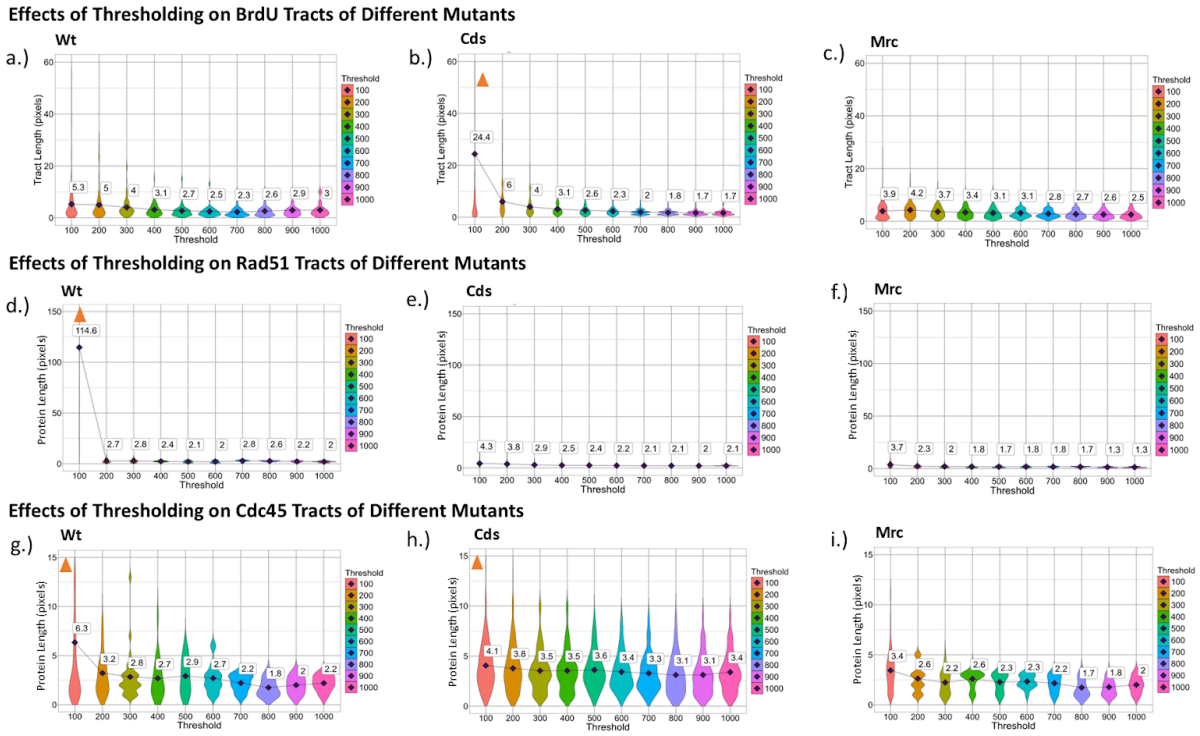

Figure 2 Increasing Thresholding Decreases BrdU, Rad51, and Cdc45 Lengths. The intensity of the line-traced chromatin fiber data was processed using R-ODD-BLOBS at different thresholds for the selected channel. The thresholds tested were 100- 1000, increasing by increments of 100. The other thresholds of the non-tested channels had a placeholder threshold initially determined by evaluating lower intensity in an initial scatter plot of the intensity as seen in S1. The preliminary baseline threshold used was 100 for DNA, 150 for BrdU, 120 for Rad51, and 130 for Cdc45. (A-C) Violin plots of the tract lengths in BrdU in wt, cds1Δ, and *mrc1Δ* at thresholds from 100- 1000. (D-F) Violin plots of the protein lengths in rad5 in wt, cds1Δ, and *mrc1Δ* at thresholds from 100- 1000. (G-I) Violin plots of the protein lengths in rad5 in wt, cds1Δ, and *mrc1Δ* at thresholds from 100- 1000. The orange triangle on the plots represents cut-off data at that threshold.

The current version, R-ODD-BLOBS first creates an initial scatter plot of the initial intensity values as seen in *S1*. We used this plot to first determine a preliminary baseline threshold, these baselines were determined by looking at the general distribution in intensity and finding a common lower limit of the majority of data for each channel. This allows for some basic low-level filtering of lower outlying data points which can skew further thresholding results. The preliminary baseline threshold determined

was 100 for DNA, 150 for BrdU, 120 for Rad51, and 130 for Cdc45. We used this preliminary baseline threshold as a placeholder when we ran the data through R-ODD-BLOBS at different thresholds for BrdU, Rad51, and Cdc45 from 100-1000.

A general trend found in all channels and conditions of thresholding is that as the threshold increases, the lengths get shorter. There also tends to be a point of saturation where the changes between thresholds become smaller. This is specifically seen in Fig 2A, where the tract length of BrdU in wt shows a slight decrease as the threshold gets larger but after the threshold of 300, the change in tract lengths is minimal. At lower thresholds like 100, in some conditions like BrdU in cds1Δ (in Fig 2B) and Rad51 in wt (Fig 2D), there's a large variation in the distribution where lengths can reach over 60 px. However, they still have a point of saturation in which changes are minimal. The lengths can also form a multimodal distribution pattern, as seen in Fig 2C,G-I, this is found in BrdU and the two proteins. These distributions can be more prominent in certain thresholds, and disappear in others. All the pattern of distribution varies, but this still has the overall general pattern of lengths decreasing as thresholds increase. However, bimodal distribution uniquely has a slight increase in mid-range thresholds and this increase varies. This is seen in the slight increase of wt Cdc45 at the threshold of 500 (as seen in Fig 2G), whereas there was a slight increase in *mrc1Δ* Cdc45 at the threshold of 400- 600 (Fig 2I). The slight increase in mid-range thresholds of multimodal distribution even occurs at the lower threshold of 300 in wt Rad51 (Fig 2D). There were also some plots with small changes between averages as seen in Fig 2C, E-F, the lengths have a small decrease when comparing the lowest threshold to the highest,

often the difference is less than 2 px (when compared to the differences in lengths in the other conditions). Although there's variation in the pattern, like multimodal distribution at different thresholding, all thresholding follows the trend of large threshold values decreasing the length in all conditions.

Smoothing Analysis using R-ODD-BLOBS

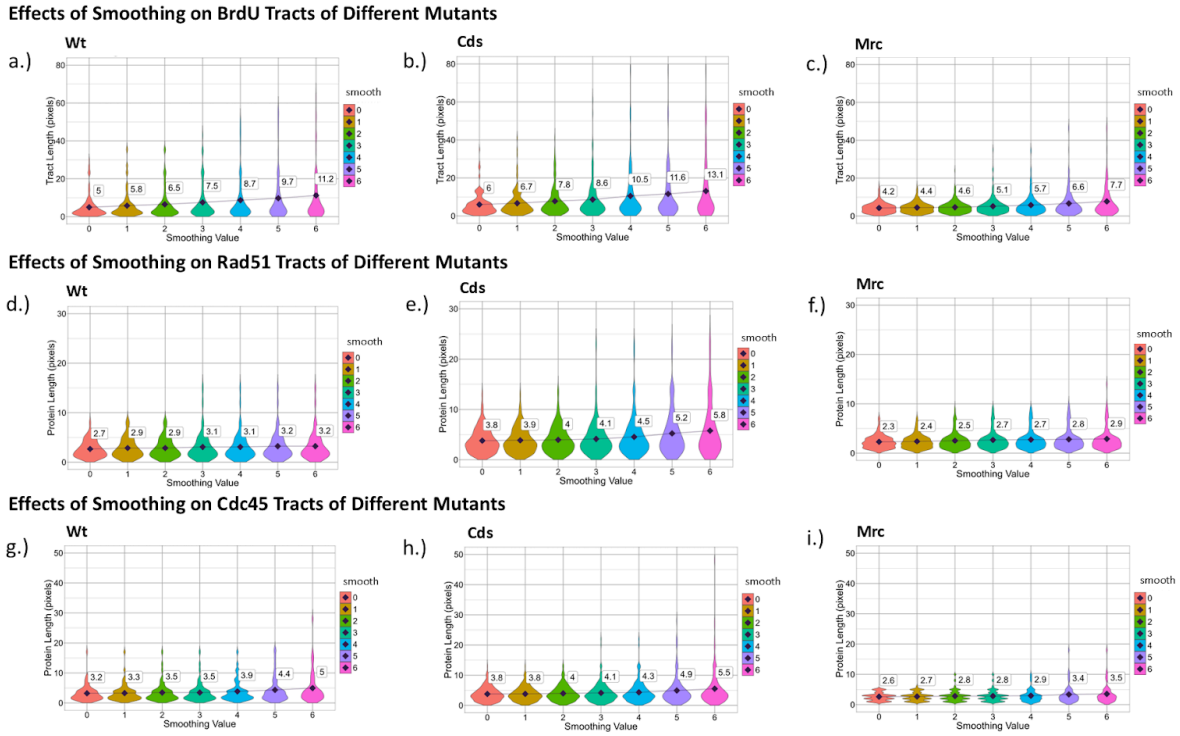

Figure 3 Larger Values of Smoothing Increases BrdU, Rad51, and Cdc45 length. The intensity of the line-traced chromatin fiber data was processed using R-ODD-BLOBS at different smoothing values from 0 to 6. The thresholds were previously determined using threshold analysis. These values were 100 for DNA, 200 for BrdU, Rad51, and Cdc45. (A-C) Violin plots of the tract lengths in BrdU in wt, *cds1Δ*, and *mrc1Δ* at smoothing values 0-6. (D-F) Violin plots of the tract lengths in Rad51 in wt, *cds1Δ*, and mrc1Δ at smoothing values 0-6. (G-I) Violin plots of the tract lengths in Cdc45 in wt, *cds1Δ*, and *mrc1Δ* at smoothing values 0-6.

Small pixel gaps between signals can be smoothed with the R-ODD-BLOBS smoothing function. This function accounts for the Abbe limit and allows the correction in the missing pixel gaps in microscopy. After thresholding values are determined using analysis (as seen in Fig 2); these values are DNA is 100, BrdU, Rad51, and Cdc45 is

200. The intensity of the line-traced chromatin fiber data was processed using R-ODD-BLOBS at different smoothing values from 0 to 6 for the BrdU, Rad51, and Cdc45 channels.

Generally, increasing smoothing values increases lengths, this increase appears to be consistent and around the same values. The change in lengths between smoothing can have a larger difference like in Fig 3A,B where the differences in the BrdU can double from initial smoothing. Smaller differences like Fig 3C-I can be less than 3px and can even be less than a difference of 1 px like in Fig 3D,F,I. If there is a multimodal pattern of distribution, a decrease in the differences in the major groups at higher smoothing can be seen (Fig 3B,G,I). As the smoothing value increases, the small groups of distribution groups at the smoothing value of 0 were “smoothed out” and the groups were not seen at higher smoothing values; this is seen in Fig 3G where the multiple groups of Cdc45 lengths were prominent from values 0- 3, and becomes smoothed and a more uniform single shape with a larger smaller length population starting at the smoothing value of 4. Smoothing affects lengths by increasing the lengths, but it also has the secondary effects of dampening and “smoothing out” groups in multimodal distribution patterns.

<u>Differences in DNA, BrdU, Rad51, and Cdc45 lengths of wt, cds1Δ and mrc1Δ</u>

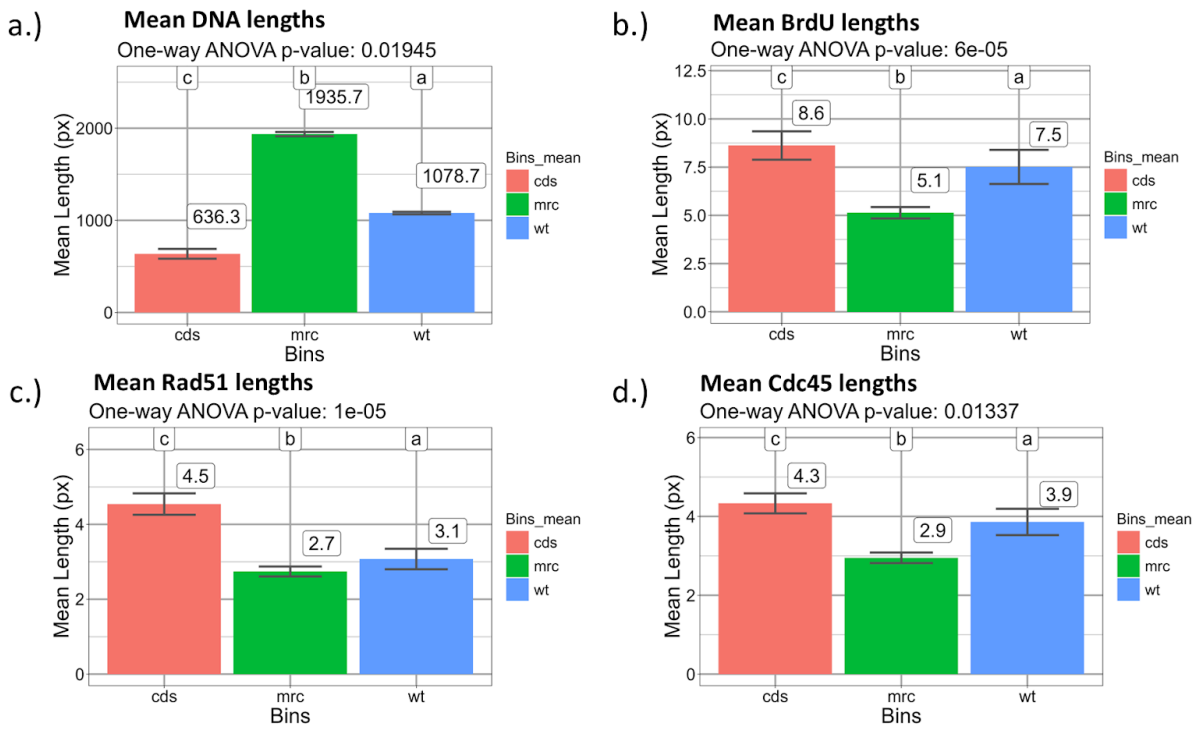

Figure 4 The Mean lengths of DNA, BrdU, Rad51, and Cdc45. The mean lengths of of DNA, BrdU, and the proteins Rad51, and Cdc45 at the thresholding and smoothing values determined by analysis (as seen in Fig 2-3) were calculated by R-ODD-BLOBS. This was done with three replicates for wt, cds1Δ, and mrc1Δ. (A) A bar graph comparing the average DNA lengths wt, cds1Δ, and mrc1Δ. (B). A bar graph comparing the average BrdU- newly synthesized lengths. (C) A bar graph comparing the average Rad51 lengths. (D) A bar graph comparing the average Cdc45 lengths. An ANOVA and Tukey HSD post hoc ($P < 0.05$) was done and each statistically different value was represented by a different letter, if there was not a significant difference then the letter would be the same.

R-ODD-BLOBS calculated the averages of the obtained lengths in each channel, thus these can be compared for each condition. The DNA lengths show the average lengths of the line-traced chromatin fiber. Each condition seen in Fig 4A showed a vastly different length and was the largest as they should represent the whole length of the fiber. The mean BrdU lengths showed statistically significant lengths where cds1Δ had the longest lengths at 8.6 px, wt had a similarly long length at 7.5 px and mrc1Δ had the shortest lengths at 5.1 px (Fig 4B). In Fig 4C, the lengths of Rad51 in each were statistically different, Rad51 in cds1Δ had the largest difference and was also the

longest at 4.5 px. Rad51 in mrc1Δ was the shortest and was nearly half the lengths of cds1Δ at 2.7 px, and wt was in between with a value of 3.1 px. In Fig 4D, Cdc45 was statistically significant and had a surprisingly similar pattern to Rad51 and had similar values. Cdc45 in cds1Δ was the longest at 4.3 px, with wt at 3.9 px, and mrc1Δ at 2.9 px. Interestingly, the pattern where cds1Δ had the longest value, wt had the mid-length, and mrc1Δ had the shortest length was seen in BrdU, Rad51, and Cdc45.

Rad51 and Cdc45 colocalization to the fork, tract, and unreplicated region

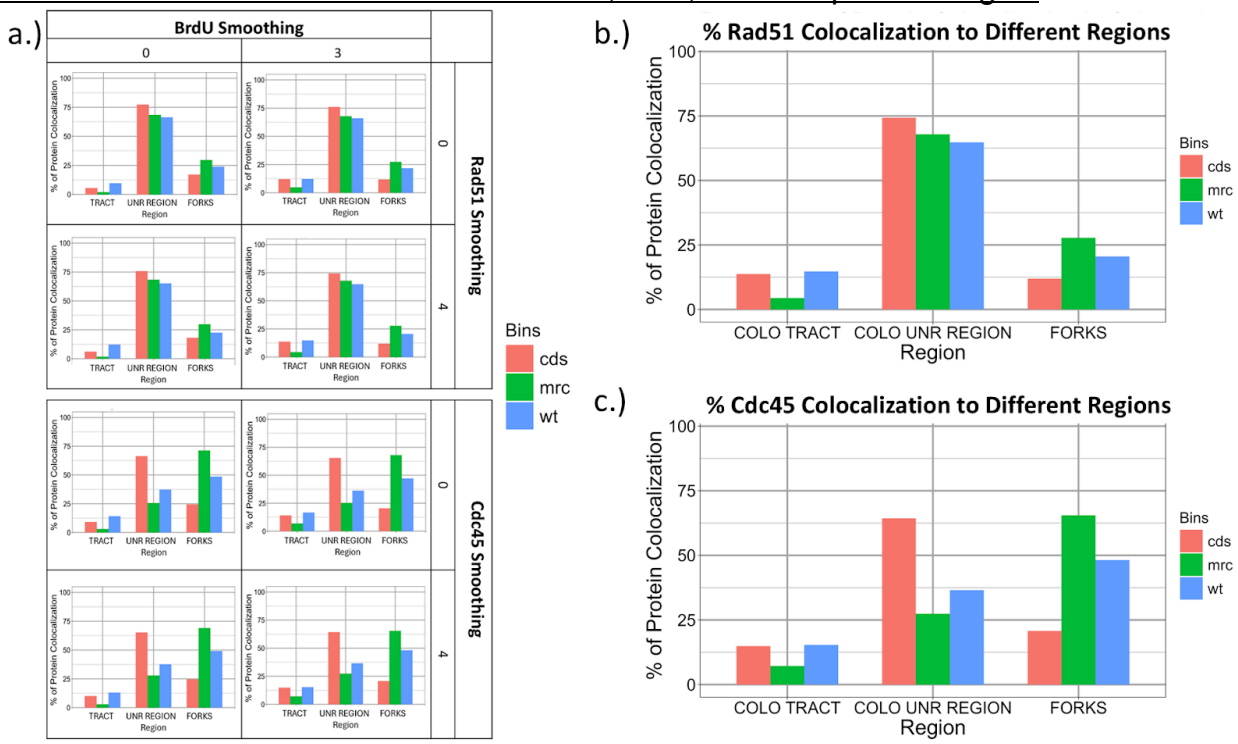

Figure 5 The BrdU and Protein Smoothing Affect Regions of Colocalization. The presence of smoothing in both BrdU and/or protein was compared in relation to each other. (A). A bar graph was used to compare the effects of zero smoothing and the determined smoothing value of 3 in BrdU and the smoothing value of 4 in both rad 51 and Cdc45. The graph illustrates the percentage of colocalization with different regions of the fiber and compares the individual relationship of smoothing on BrdU or protein alone and together. (B) A bar graph that compares the percentage of Rad51 colocalization to the tract, unreplicated region and fork at the determined baseline threshold and smoothing. (B) A bar graph that compares the percentage of Cdc45 colocalization to the tract, unreplicated region and fork at the determined baseline values.

As the smoothing function can smooth in small gaps, proteins that filament like Rad51 can also be smoothed and this can affect colocalization. The effects of the presence of smoothing of BrdU and protein can change the categorization of protein-region colocalization by R-ODD-BLOBS. This effect of smoothing can be individual, or together, so we explored the relationship of BrdU and protein smoothing. The determined smoothing baseline was used (BrdU= 3, Rad51= 4, Cdc45= 4) with variations of which values were zero. The colocalization remained quite similar whether smoothing was applied or not in both BrdU and/or protein (as seen in Fig 5a). When comparing BrdU smoothing, in the presence of BrdU smoothing, both Rad51 and Cdc45 show a slight decrease in the percentage of cds1Δ fork colocalization while the percentage of cds1Δ tract colocalization increases. This slight decrease in fork colocalization change is also seen when there's protein (Rad51 or Cdc45) smoothing but at a smaller scale.

As the effects of smoothing on colocalization were minimal, the previously determined baseline values remained the same and were applied to the data. The majority of Rad51 in Fig 5B were at unreplicated regions; cds1Δ had the most, and wt had the least. Around 10- 28% of Rad51 were colocalized at the fork, with mrc1Δ having nearly double the proportion in comparison to cds1Δ. Colocalization at the tract was the smallest proportion at around 3-15%, where mrc1Δ has the least and wt and cds1Δ have similar proportions. The percentage of cds1Δ at the tract and fork are similar at around 20%, and this is also seen with wt as the colocalization is around 20%. In Fig

5C, the percentage of Cdc45 colocalization at the baseline was also obtained. Here the unreplicated regions and fork colocalization proportions are similar with a wide range from 20- 65%. In the unreplicated region cds1Δ, again, had the largest percentage, wt had less, and mrc1Δ had the least and was nearly half the percentage. This unreplicated region colocalization pattern of Cdc45 was seen inversely in the fork region, conditions in which there were low amounts in the unreplicated region were high in forks. So, mrc1Δ had the highest percentage in forks, with wt having similar amounts to the unreplicated regions, and cds1Δ having the least amount of colocalization (when compared to the other conditions). In all conditions, there was low colocalization at the tracts with cds1Δ and wt having similar percentages, and mrc1Δ being the lowest at around 6%.

Adjusting the fork window (number of unreplicated fork regions x number of replicated fork regions) can allow you to explore proteins near the fork

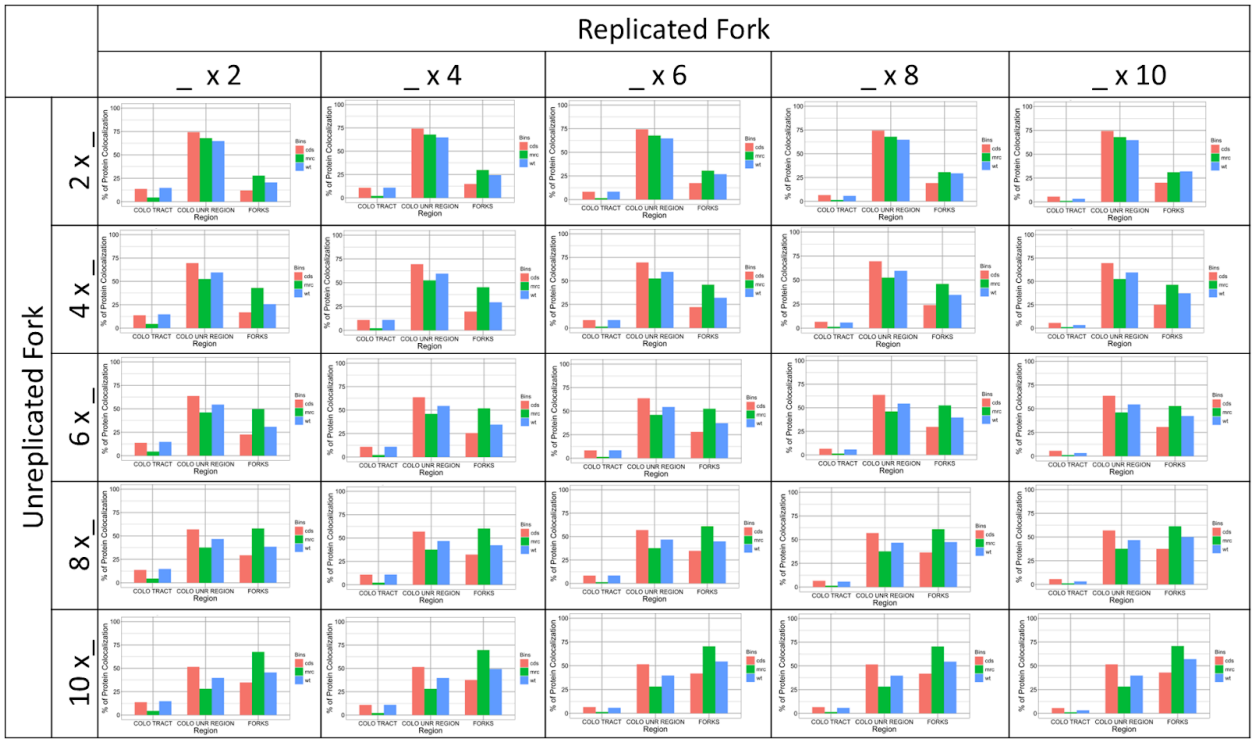

Figure 6 Changing the Number of Replicated and Unreplicated Fork Pixels Can Suggest the Presence of HR. The multiple-grouped bar graph compares the effects of pixel designation of unreplicated and replicated forks on Rad51-region colocalization. As the grid goes from up to down, the number of pixels in the unreplicated fork increases from 2- 10 in increments of 2. As the grid goes from left to right, the number of pixels in the replicated fork increases from 2- 10 in increments of 2.

A feature of R-ODD-BLOBS is the ability for users to define the number of pixels in replicated regions of the fork, the region of the fork where replication is occurring and has passed, and the number of pixels in the unreplicated region of the fork, this would be the opposite side where is unravelling and the direction the fork is moving. This feature gives the user an idea of nearby proteins and allows for the accommodation of different fork anatomy. The increase in designated replication fork shows an increase in fork colocalization as seen in Fig 6. Interestingly, as the designation number of pixels in the unreplicated fork increases, colocalization in unreplicated regions decreases, and

fork colocalization increases. The unreplicated fork region at 2 pixels showed cds1Δ had 74% colocalization, mrc1Δ had 67%, and wt had 64%. By only increasing the unreplicated region by 8 pixels to 10 pixels, cds1Δ colocalization decreased 23% to 51%, mrc1Δ decreased by 39% to 28%, and wt decreased by 24% to 40%. Conjunctly, the fork region at an unreplicated fork region at 2 pixels showed cds1Δ had only 12%, mrc1Δ had 27%, and wt had 21%. When increasing the unreplicated fork region to 10 pixels, cds1Δ increased by 23% to 35%, mrc1Δ increased by 41% to around 68%, and wt increased by 25% to 46%

DISCUSSION

ODD-BLOBS to R-ODD-BLOBS

These studies pointed to the potential power of chromatin fibers to analyze replication tracts and associations. Proteins may be monitored within a defined region to model the replication fork. This can be used to assess heterogeneity across a population of replication forks and to define mutant fork structures and protein or synthesis relationships in new ways. The first iteration of ODD-BLOBS was a VBA script, the script was able to analyze intensity data within an Excel and obtain the length, and protein colocalization at the fork as seen in Fig 1 B,D. This method remains faster than manual analysis and provides useful information on lengths of signal and protein-region colocalization data. However, with the use of this tool, there were concerns about the stability of the script, as it could be clunky and a bit slow in larger data sets. We decided that translating this program so that its based in the programming language R, could help mitigate these concerns. R-ODD-BLOBS is this

said version; it has the same previous features like obtaining tract length, determining protein-region colocalization (eg. fork, or tract), and the ability to change parameters like thresholding for each channel, smoothing for each channel, and changing the number of designated unreplicated and replicated fork pixels. The additional feature is the creation of individual and binned (the average of multiple replicates) graphs of protein-region colocalization (the binned version can be seen in Fig 5 and 6), the binned mean lengths of each channel (seen in Fig 4), as well as the length of each channel compared to each sheet, and initial scatter plots (seen in S1). The creation of these graphs can help users quickly identify patterns within their data and potentially facilitate data analysis.

Validation of R-ODD-BLOBS Program

The threshold analysis and smoothing analysis allowed us to determine systematically a threshold and smoothing value. Certain patterns in thresholding where there was a clear saturation in lengths and a reduction in changes between upper thresholds (example in Fig 2A) allow us to determine a clear threshold that could be used. However, this thresholding is averaged, and when we look at the thresholding of individual replicates (S2-4), there is variety in the distribution of ranges which could suggest different replicates may work better with another threshold. However, the average does serve the purpose of finding the best overall threshold of all the replicates. Smoothing had a general increasing pattern which reduces the distinction between multimodal distribution patterns. Although this pattern was hard to determine the best value, we were cautious of large changes due to smoothing, whether it could be a large increases in length or if the distribution was completely erased, we saw this in both the average smoothing in Fig 3, and as well as in S5-7. We used the Abbe limit

in conjunction to determine the best smoothing value. By considering the limits of light emitted from fluorescent microscopy, we calculated what is the limit of resolution. For example, when using a green light (488 nm) and NA for the system (1.4), it was determined that signals less than 3 pixels apart cannot be discriminated against. As a result, the standard smooth value used was 3 pixels for this channel.

The analysis also allows us to access the functionality of the R-ODD-BLOBS program. In thresholding, we can hypothesize that if we increase the value in which numbers (in this case this is the intensity of each pixel) that do not reach this value are excluded we would see a decrease in lengths. We can also hypothesize that there are likely lower intensity values that can contribute to the length and skew the results. Once we filter that out with thresholding and reach the majority data, we should be able to see a saturation in values, and minimal changes between thresholds. From Fig 2, we do see this result from the general decreasing value, as well as the saturation point in some cases. This suggests that the program is running as intended. For smoothing we hypothesize that accounting for the Abbe limit in microscopes would connect lengths with small gaps into longer lengths. We saw this trend in all our smoothing figures (Fig 3, S5-7).

Newly Synthesized DNA and Protein Lengths

There are significant differences between the mean lengths of BrdU in wt, cds1Δ and mrc1Δ, as seen in Fig 4B. mrc1Δ is the shortest at 5.1 px, cds1Δ are the longest at 8.6 px, and wt is right behind at 7.5 px. This trend is comparable to literature where cds1Δ were the longest, followed by wt and then mrc1Δ which was less than half of

cds1Δ (Sabatinos *et al.*, 2012) after a 45 min release from HU. This would continue to support that mrc1Δ is sensitive to DNA damage from HU and quickly collects stalled forks and fails to recover, as early as 30 mins after release. This was primarily suggested to be due to the absence of mrc1Δ leading to the uncoupling of the replisome machinery, and thus replication at the fork is stalled leading to truncated replication (Sabatinos *et al.*, 2012).

When comparing each protein in the different strains the difference is significant, although interestingly the the lengths and patterns in both Rad51 and Cdc45 are similar, as seen in Fig 4C,D. cds1Δ have the longest protein lengths for Rad51 and Cdc45 at lengths of 4.5 and 4.3 px respectively. Wt has the second longest protein lengths, where Rad51 is 3.1 px, and Cdc45 is 3.9 px. The shortest is mrc1Δ, where Rad51 is 2.7 px, and Cdc45 is 2.9 px. This could potentially suggest thresholding can be adjusted, and when looking at the thresholds of Cdc45 in Fig 2G-I, we can see there are more frequency appearances of multimodal distribution, which has the potential to skew the lengths to be larger at certain thresholds.

<u>Cdc45 Colocalization</u>

Cdc45 is a protein that is coupled with Mcm2-7 and GINS to create the CMG complex that unwinds dsDNA during replication (Petojevic *et al.*, 2015). Thus, this protein would be found often in the fork, this is reflected in our colocalization results (Fig 5C), where a large portion of Cdc45 in wt and *mrc1Δ* is found in the fork. Interestingly, Cdc45 in cds1Δ has the highest colocalization in unreplicated regions. Cdc45 can colocalize at unreplicated regions, specifically at replication origins and this can allow

for the timing of firing (Tanaka *et al.*, 2011). However, it's also found to associate with non-origin DNA when pre-replication complexes are destroyed (Aparicio *et al.*, 1997). Depending on the phase of the *cds1Δ* cells, either possibility could have caused an increased colocalization to unreplicated regions.

Rad51 Colocalization and HR

The structure of a fork and its parameters is loosely defined. Thus, we included a feature where the user can define this "fork window" region by the designation of pixels in the unreplicated and replicated part of the forks; alongside the initial one fork pixel (if the unreplicated and replicated fork pixel is 2, then the total number of fork regions is 5 pixels). The process of R-ODD-BLOBS calculating colocalization is first done by labelling whether a pixel associated with protein is colocalized at the fork, tract, or unreplicated region. One of the downsides of this iteration is that proteins that can filament and span over multiple regions can be recognized as multiple different proteins that are beside each other. However, the protein colocalization feature calculates the proportion by the number of "colocalization region labels" in pixels to the total amount of protein in pixels. So the proportion would remain accurate for most proteins that occur at a small point like Cdc45, but the interactions in filamentous proteins like Rad51 would be truncated and lost. We counteracted this by increasing and decreasing the number of designated unreplicated and replicated fork pixels. This allows us to label more nearby protein pixels with the "colocalization at fork" label which allows us to detect proteins that are beside the fork and potentially connected (filamented) through a higher percentage of colocalization at the fork region.

As this feature would mainly affect protein colocalization, expansive forks would allow for more allocation to the fork region and less in the unreplicated region and tract. A baseline value for the forks can arguably be a conservative number of pixels like 1 or 2, allowing for tight regulation and thresholding of what proteins are categorized as “fork colocalized”. However, as it’s user-defined, this feature is flexible and can allow users to explore and accommodate different fork anatomies. An example would be a chicken foot structure by increasing the number of replicated forks, this can allow for the detection of proteins on the end of the chicken foot and what is contributing to the structure formation. This can also allow us to explore proteins near the fork by increasing the number of pixels in the unreplicated or replicated region of the fork. In the case of Rad51, as it is a nucleoprotein that filaments on ssDNA from double-strand breaks (Carver and Zhang, 2021) it can filament in the fork and into the replicated or unreplicated region suggesting different types of structures. The Rad51 protein around the fork was explored due to its nature to filament. In Fig 6, the increase of 8 pixels in the unreplicated fork region led to a notable decrease in Rad51 colocalization in unreplicated regions. Colocalization in the unreplicated region by cds1Δ decreased by 23%, *mrc1Δ* decreased by 39%, and wt decreased by 24%. Whereas colocalization at the forks region increased in cds1Δ by 23%, mrc1Δ by 41%, and wt by 25%, with the difference between the condition with the highest colocalization, *mrc1Δ*, and the second, wt, being 22%. The similarities between *cds1Δ* and wt in Rad51 protein colocalization suggest that replication fork and stall have not occurred 30 minutes after release of HU. The late origin firing, and DNA unwinding (Sabatinos *et al.*, 2012), found in the response of cds1Δ to HU have likely not occurred yet, and would suggest that it’s

acting like wt, which is relatively insensitive to HU. There was also some increase, at around 10% colocalization to forks when the replication fork regions pixels are increased, although this isn't a lot in comparison, some appearances of Rad51 within the fork and onto the tract can occur when Rad51 filaments. This suggests that Rad51 proteins are near the fork (within 8 pixels) and likely recruited for a function. HR is a mechanism that is used to repair stalled forks and is the catalyst of the homology search for DNA strand exchange (Li and Heyer, 2008) by Rad51. This increased colocalization at the fork can potentially suggest that Rad51 is recruited to repair stalled forks from HU damage. Also, when this is compared to Cdc45, there is an increase in fork colocalization in increasing the designation of unreplicated fork pixels. But this increase is not as large as the 41% increase of *mrc1Δ*, and the change is around 20% and less, as seen in S8. This smaller change supports the idea that Rad51 specifically colocalizes to forks in *mrc1Δ*, potentially due to mechanisms like being in play.

When compared to the literature, Rad51 *in vivo* assembles into a filament on RPA to coat ssDNA during HR (Taylor *et al.*, 2015). Our data in Fig 6 reflects this and shows Rad51 colocalization to the fork and unreplicated regions, with higher values of unreplicated fork regions showing the Rad51 proteins in the unreplicated regions, are near the fork suggest filaments. Rad51 may also bind to both ssDNA and dsDNA which suggests that the filamentation from fork to nearby unreplicated regions containing dsDNA. This observation supports the regions of colocalization we saw. In addition, DNA damage-sensitive conditions like mrc1Δ in which the loss of *mrc1Δ* leads to the destabilization of the replication fork (fork stalling) and leads to ssDNA accumulation

(Sabatinos *et al.*, 2012) had a large increase in fork colocalization at 41% which suggests the HR repair pathway might have been recruited to save these stalled forks. The short *mrc1Δ* BrdU lengths of 5.1 px in Fig 4B also suggest that the forks have been stalled since HU treatment. The increase of fork colocalization in wt and cds1Δ are similar (25% and 23%, respectively). This likely suggests that there are fewer stalled forks, and the presence of longer BrdU lengths in wt and *cds1Δ* (seen in Fig 4B), supports this. This is likely due to the functional *mrc1Δ1* protein in the *cds1Δ* mutant, which allows for helicase and polymerase to continue to be linked which allows for replication (and therefore the forks are not stalled) (Sabatinos *et al.*, 2012). The colocalization data we collect suggests that we detected HR with Rad51; further studies with tagging rad52 (a mediator of Rad51 in yeast (Benson *et al.*, 1998)) and determining colocalization can be done to further confirm that HR is occurring.

MATERIALS & METHODS

We used wildtype, *mrc1Δ,* and cds1Δ yeast cell strains that express the transgene of *hsv-tk* and *hENT1* for the experiments (as previously described in (Sabatinos *et al.*, 2012). The cells were grown in BrdU to prepare for chromatin fiber stretching. We also labelled the fixed cells with immunofluorescent DAPI, anti-BrdU antibodies, Rad51 and, Cdc45. We then imaged the cells using a Deltavision Spectris microscope equipped with a 1.4 NA, 63x oil immersion lens, resulting in z-section stacks. Three chromatin fiber images of each strain were collected, totalling nine

images. Further details of data collection through chromatin microscopy can be found in the supplementary.

The chromatin fiber images were manually traced, and these line-traced fibers were obtained by the DeltaVision microscope with softWoRx v4.1 (GE, Issaquah, WA) using a 60x (NA1.4 PlanApo) lens, solid-state illuminator and 12-bit CCD camera. Images were acquired in five 0.2μm z-sections, then deconvolved and Maximum Intensity Projected (softWoRx, default settings). We then ran the intensity data in R-ODD-BLOBS to obtain the initial scatter plot data to determine the preliminary baseline threshold before re-running R-ODD-BLOBS from 100- 1000, increasing by increments of 100. The best thresholding values for this data are DNA is 100, and BrdU, Rad51 and Cdc45 is 200. After thresholding was confirmed, we did a smoothing effects analysis, where we re-ran R-ODD-BLOBS with the thresholds while testing smoothing values from 0-6. The best smoothing value for this data is DNA and BrdU is 3, and both proteins are 4. After the threshold and smoothing were determined the R-ODD-BLOBS was run with these values to determine protein colocalization within each region (i.e. unreplicated, fork, replicated) and (DNA, BrdU, and protein) lengths. Further details can be found in Supplementary.

REFERENCES

Alabert, C, Bianco, JN, and Pasero, P (2009). Differential regulation of homologous recombination at DNA breaks and replication forks by the mrc1 branch of the S-phase

checkpoint. EMBO J 28, 1131–1141.
Aparicio, OM, Weinstein, DM, and Bell, SP (1997). Components and Dynamics of DNA Replication Complexes in S. cerevisiae: Redistribution of MCM Proteins and Cdc45p during S Phase. Cell 91, 59–69.
Benson, FE, Baumann, P, and West, SC (1998). Synergistic actions of Rad51 and Rad52 in recombination and DNA repair. Nature 391, 401–404.
Bonilla, B, Hengel, SR, Grundy, MK, and Bernstein, KA (2020). RAD51 Gene Family Structure and Function. Annu Rev Genet 54, 25–46.
Calzada, A, Hodgson, B, Kanemaki, M, Bueno, A, and Labib, K (2005). Molecular anatomy and regulation of a stable replisome at a paused eukaryotic DNA replication fork. Genes Dev 19, 1905.
Carver, A, and Zhang, X (2021). Rad51 filament dynamics and its antagonistic modulators. Semin Cell Dev Biol 113, 3–13.
Daigaku, Y, Keszthelyi, A, Müller, CA, Miyabe, I, Brooks, T, Retkute, R, Hubank, M, Nieduszynski, CA, and Carr, AM (2015). A global profile of replicative polymerase usage. Nat Struct Mol Biol 22, 192–198.
Errico, A, Cosentino, C, Rivera, T, Losada, A, Schwob, E, Hunt, T, and Costanzo, V (2009). Tipin/Tim1/And1 protein complex promotes Polα chromatin binding and sister chromatid cohesion. EMBO J 28, 3681.
Feng, W, Collingwood, D, Boeck, ME, Fox, LA, Alvino, GM, Fangman, WL, Raghuraman, MK, and Brewer, BJ (2006). Genomic mapping of single-stranded DNA in hydroxyurea-challenged yeasts identifies origins of replication. Nat Cell Biol 8, 148–155.
Hyrien, O (2000). Mechanisms and consequences of replication fork arrest. Biochimie 82, 5–17.
Kemp, MG, Akan, Z, Yilmaz, S, Grillo, M, Smith-Roe, SL, Kang, T-H, Cordeiro-Stone, M, Kaufmann, WK, Abraham, RT, Sancar, A, *et al.* (2010). Tipin-Replication Protein A Interaction Mediates Chk1 Phosphorylation by ATR in Response to Genotoxic Stress. J Biol Chem 285, 16562.
Koç, A, Wheeler, LJ, Mathews, CK, and Merrill, GF (2004). Hydroxyurea arrests DNA replication by a mechanism that preserves basal dNTP pools. J Biol Chem 279, 223–230.
Lambert, S, Froget, B, and Carr, AM (2007). Arrested replication fork processing: Interplay between checkpoints and recombination. DNA Repair 6, 1042–1061.
Lee, J, Gold, DA, Shevchenko, A, Shevchenko, A, and Dunphy, WG (2005). Roles of Replication Fork-interacting and Chk1-activating Domains from Claspin in a DNA Replication Checkpoint Response. Mol Biol Cell 16, 5269–5282.
Li, X, and Heyer, W-D (2008). Homologous recombination in DNA repair and DNA damage tolerance. Cell Res 18, 99–113.
Lou, H, Komata, M, Katou, Y, Guan, Z, Reis, CC, Budd, M, Shirahige, K, and Campbell, JL (2008). mrc1 and DNA polymerase ε function together in linking DNA replication and the S phase checkpoint. Mol Cell 32, 106.
Nedelcheva, MN, Roguev, A, Dolapchiev, LB, Shevchenko, A, Taskov, HB, Shevchenko, A, Francis Stewart, A, and Stoynov, SS (2005). Uncoupling of Unwinding from DNA Synthesis Implies Regulation of MCM Helicase by Tof1/mrc1/Csm3 Checkpoint Complex. J Mol Biol 347, 509–521.
Nitani, N, Yadani, C, Yabuuchi, H, Masukata, H, and Nakagawa, T (2008). Mcm4

C-terminal domain of MCM helicase prevents excessive formation of single-stranded DNA at stalled replication forks. Proc Natl Acad Sci 105, 12973–12978.
Noguchi, E, Noguchi, C, McDonald, WH, John R Yates, III, and Russell, P (2004). Swi1 and Swi3 Are Components of a Replication Fork Protection Complex in Fission Yeast. Mol Cell Biol 24, 8342.
O'Donnell, M, and Li, H (2016). The Eukaryotic Replisome Goes Under the Microscope. Curr Biol CB 26, R247.
Oijen, AM van (2007). Single-molecule studies of complex systems: the replisome. Mol Biosyst 3, 117–125.
Pacek, M, and Walter, JC A requirement for MCM7 and Cdc45 in chromosome unwinding during eukaryotic DNA replication. EMBO.
Petojevic, T, Pesavento, JJ, Costa, A, Liang, J, Wang, Z, Berger, JM, and Botchan, MR (2015). Cdc45 (cell division cycle protein 45) guards the gate of the Eukaryote Replisome helicase stabilizing leading strand engagement. Proc Natl Acad Sci 112, E249–E258.
Rozenzhak, S, Mejía-Ramírez, E, Williams, JS, Schaffer, L, Hammond, JA, Head, SR, and Russell, P (2010). Rad3ATR Decorates Critical Chromosomal Domains with γH2A to Protect Genome Integrity during S-Phase in Fission Yeast. PLOS Genet 6, e1001032.
Sabatinos, SA, Forsburg, SL, Sabatinos, SA, and Forsburg, SL (2013a). Preserving the Replication Fork in Response to Nucleotide Starvation: Evading the Replication Fork Collapse Point. In: The Mechanisms of DNA Replication, IntechOpen.
Sabatinos, SA, Green, MD, and Forsburg, SL (2012). Continued DNA Synthesis in Replication Checkpoint Mutants Leads to Fork Collapse. Mol Cell Biol 32, 4986–4997.
Sabatinos, SA, Mastro, TL, Green, MD, and Forsburg, SL (2013b). A Mammalian-Like DNA Damage Response of Fission Yeast to Nucleoside Analogs. Genetics 193, 143–157.
Sirbu, BM, Couch, FB, Feigerle, JT, Bhaskara, S, Hiebert, SW, and Cortez, D (2011). Analysis of protein dynamics at active, stalled, and collapsed replication forks. Genes Dev 25, 1320–1327.
Snyder, RD (1984). The role of deoxynucleoside triphosphate pools in the inhibition of DNA-excision repair and replication in human cells by hydroxyurea. Mutat Res 131, 163–172.
Sogo, JM, Lopes, M, and Foiani, M (2002). Fork reversal and ssDNA accumulation at stalled replication forks owing to checkpoint defects. Science 297, 599–602.
Stratmann, SA, and Oijen, AM van (2014). DNA replication at the single-molecule level. Chem Soc Rev 43, 1201–1220.
Szyjka, SJ, Viggiani, CJ, and Aparicio, OM (2005). mrc1 Is Required for Normal Progression of Replication Forks throughout Chromatin in S. cerevisiae. Mol Cell 19, 691–697.
Tanaka, H, Katou, Y, Yagura, Saitoh, K, Itoh, T, Araki, H, Bando, M, and Shirahige, K (2009). Ctf4 coordinates the progression of helicase and DNA polymerase α - Tanaka - 2009 - Genes to Cells - Wiley Online Library. Genes Cells.
Tanaka, S, Nakato, R, Katou, Y, Shirahige, K, and Araki, H (2011). Origin Association of Sld3, Sld7, and Cdc45 Proteins Is a Key Step for Determination of Origin-Firing Timing. Curr Biol 21, 2055–2063.
Taylor, MR, Špírek, M, Chaurasiya, KR, Ward, JD, Carzaniga, R, Yu, X, Egelman, EH,

Collinson, LM, Rueda, D, Krejci, L, *et al.* (2015). Rad51 Paralogs Remodel Pre-synaptic Rad51 Filaments to Stimulate Homologous Recombination. Cell 162, 271.
Walter, J, and Newport, J (2000). Initiation of Eukaryotic DNA Replication: Origin Unwinding and Sequential Chromatin Association of Cdc45, RPA, and DNA Polymerase α. Mol Cell 5, 617–627.
Yurieva, O, and O'Donnell, M (2016). Reconstitution of a eukaryotic replisome reveals the mechanism of asymmetric distribution of DNA polymerases. Nucleus 7, 360.

TABLES

Strain	Genotype	Source
wt	*h+ rad11myc::KanMX cdc45-YFP-ura4+ leu1-32::hENT1-leu1+(pJAH29) his7-366::hsv-tk-his7+(pJAH31) ura4-D18 ade6-M210*	FY 3805*
mrc1Δ	*h- Δmrc1::ura4+ cdc45-YFP-ura4+ leu1-32::hENT1-leu1+(pJAH29) his7-366::hsv-tk-his7+(pJAH31) rad11myc::KanMX ura4-D18 ade6-M210*	FY 3821
cds1Δ	*h- Δcds1::ura4+ cdc45-YFP-ura4+ rad11myc::KanMX leu1-32::hENT1-leu1+(pJAH29) his7-366::hsv-tk-his7+(pJAH31) ura4-D18 ade6-M210 (rad11=ssb1)*	FY 3830

*SL Forsburg, University of Southern California

FIGURE LEGENDS

Figure 1: Figure 1 Previous data analysis of wt, cds1Δ and mrc1Δ on polα using ODD-BLOBS.
Figure 2: Increasing Thresholding Decreases BrdU, Rad51, and Cdc45 Lengths
Figure 3: Larger Values of Smoothing Increases BrdU, Rad51, and Cdc45 length.
Figure 4: The Mean lengths of DNA, BrdU, Rad51, and Cdc45.
Figure 5: The BrdU and Protein Smoothing Affect Regions of Colocalization.
Figure 6: Changing the Number of Replicated and Unreplicated Fork Pixels Can Suggest the Presence of HR.
Supplemental Figure 1: Initial Scatter Plot of Channel intensities of One WT file

Supplemental Figure 2: Individual Replicates of BrdU Thresholding for Wt, cds1Δ and mrc1Δ.
Supplemental Figure 3: Individual Replicates of Rad51 Thresholding for Wt, cds1Δ and mrc1Δ.
Supplemental Figure 4: Individual Replicates of Cdc45 Thresholding for Wt, cds1Δ and mrc1Δ.
Supplemental Figure 5: Individual Replicates of BrdU Smoothing for Wt, cds1Δ and mrc1Δ.
Supplemental Figure 6: Individual Replicates of Rad51 Smoothing for Wt, cds1Δ and mrc1Δ.
Supplemental Figure 7: Individual Replicates of Cdc45 Smoothing for Wt, cds1Δ and mrc1Δ.
Supplemental Figure 8: Effects of Replication Window on Cdc45 colocalization
Supplemental Figure 9: ODD-BLOBS Rad51 and Cdc45 colocalization

SUPPLEMENTAL FIGURES

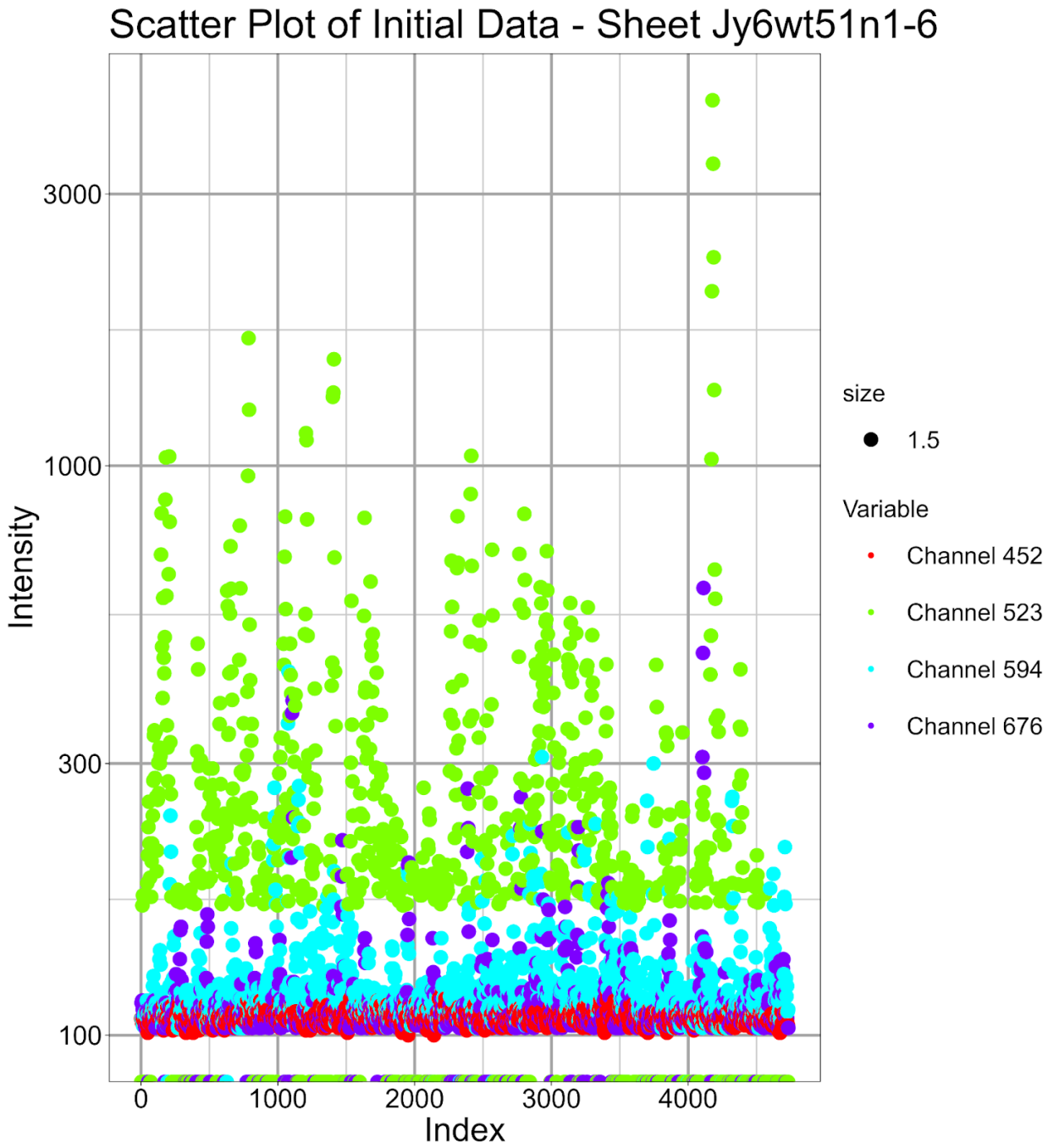

S1 Initial Scatter Plot of Channel intensities of One WT file. One of the R-ODD-BLOBS outputs is a scatter plot of the intensities of each channel on a log10 intensity value scale. This allows users to determine trends in intensities for each channel and lower limits. Channel 452 is DNA and is represented by the red points, it shows a general trend of having an intensity value of around 100-200. Channel 523 is BrdU and is represented by the green points, it shows a wider range of around 150 to the upper limits of the scale of 5400. Channel 594 is Rad51 and is represented by the cyan points, it shows a mid-range of around 120- 300 intensity. Channel 676 is Cdc45

and is represented by the purple points, it shows a mid-range of around 130- 550. Due to the clear lower limits of each channel, this allows us to use the temporary placeholder thresholding of DNA as 100, BrdU as 150, Rad51 as 120, and Cdc45 for thresholding analysis.

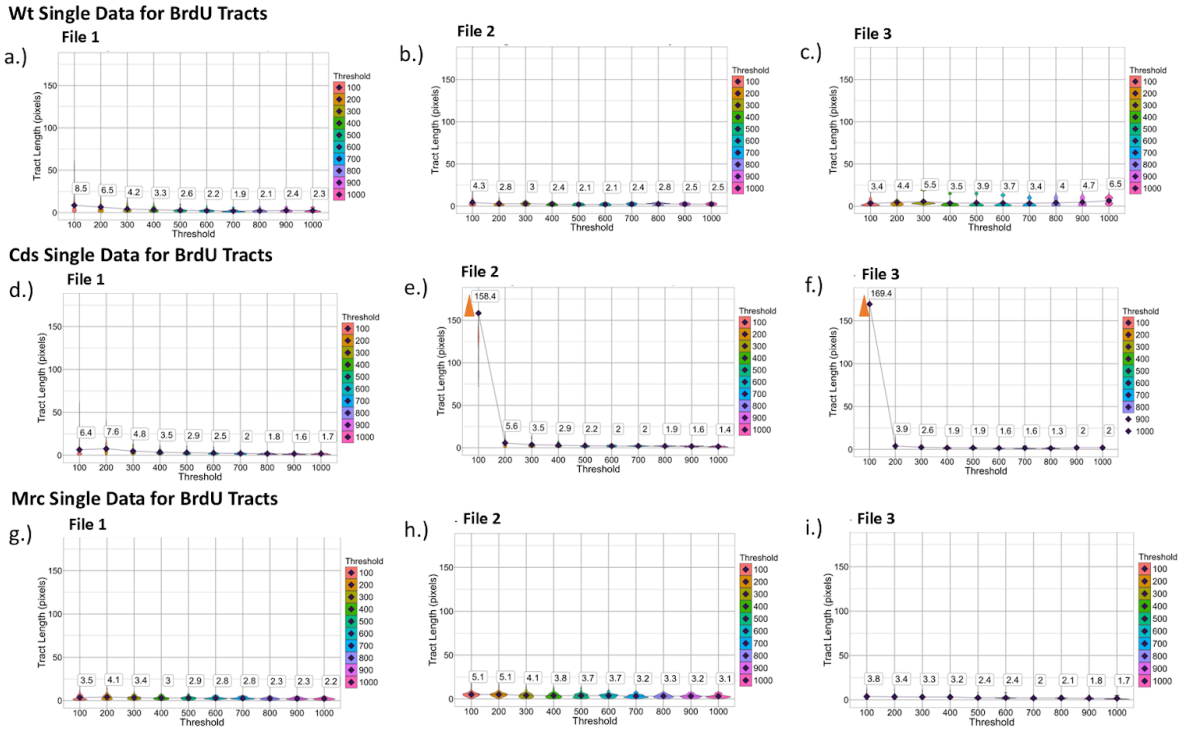

S2 Individual Replicates of BrdU Thresholding for Wt, *cds1Δ* and *mrc1Δ*. The individual BrdU lengths at the image slides of the three replicates of wt, *cds1Δ*, and mrc1Δ. (A-C) The violin plot shows different thresholds' effects on the three wt replicates. (D-F) The violin plot shows different thresholds' effects on the three *cds1Δ* replicates. (G-I) The violin plot shows different thresholds' effects on the three *mrc1Δ* replicates.

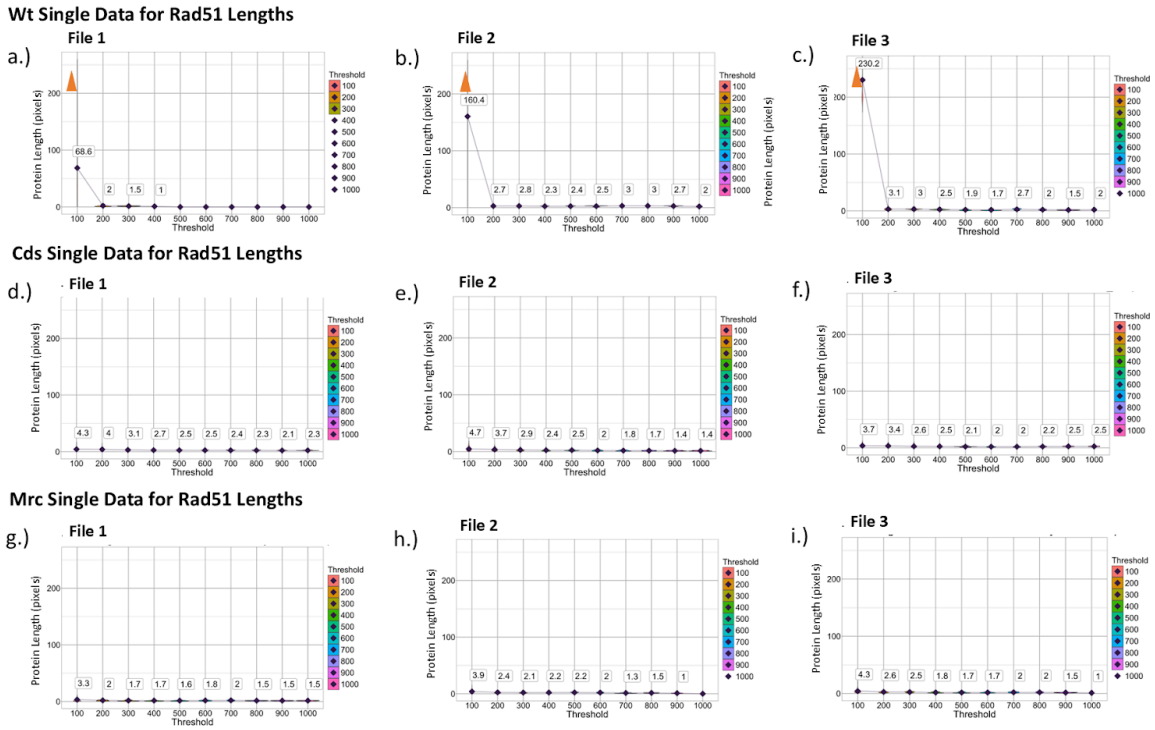

S3 Individual Replicates of Rad51 Thresholding for Wt, *cds1Δ* and *mrc1Δ*. The individual Rad51 protein lengths at the image slides of the three replicates of wt, *cds1Δ*, and *mrc1Δ*. (A-C) The violin plot shows different thresholds effects on the three wt replicates. (D-F) Threshold effects on the three *cds1Δ* replicates. (G-I) Thresholds effects on the three *mrc1Δ* replicates.

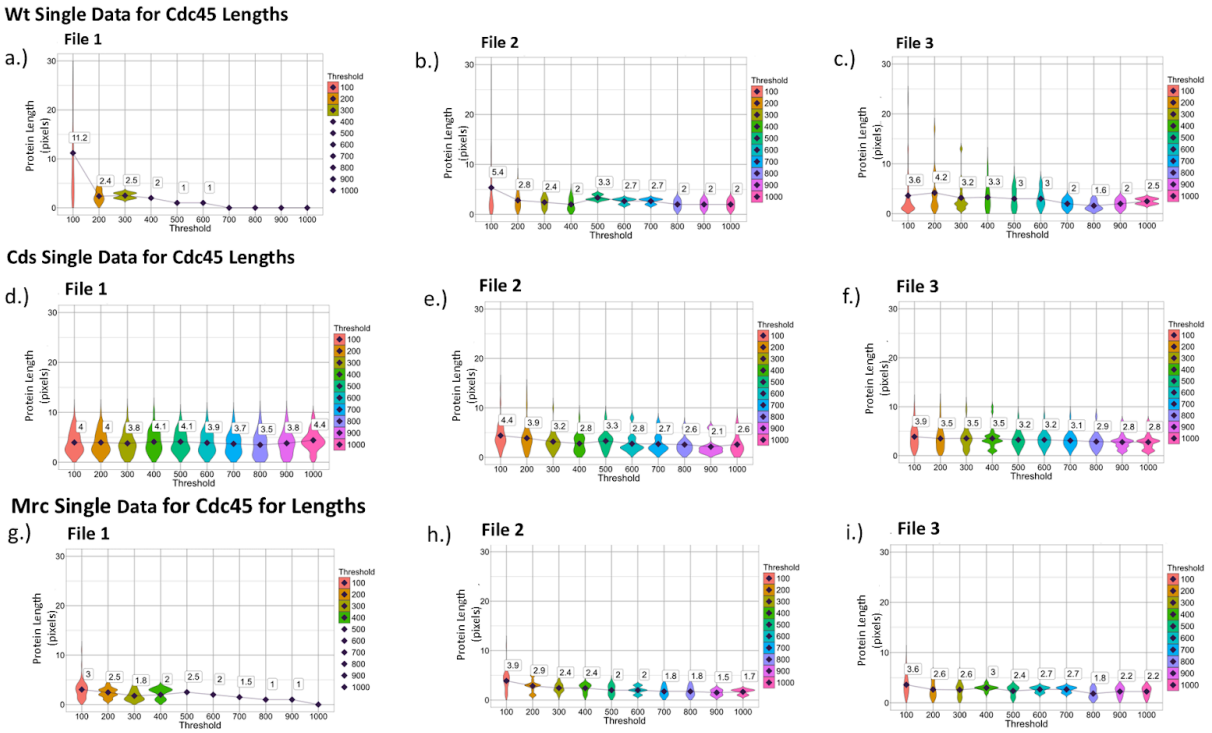

S4 Individual Replicates of Cdc45 Thresholding for Wt, cds1Δ and mrc1Δ. The individual Cdc45 protein lengths at the image slides of the three replicates of wt, cds1Δ, and mrc1Δ. (A-C) The violin plot shows different thresholds' effects on the three wt replicates. (D-F) The violin plot shows different thresholds' effects on the three cds1Δ replicates. (G-I) The violin plot shows different thresholds' effects on the three mrc1Δ replicates.

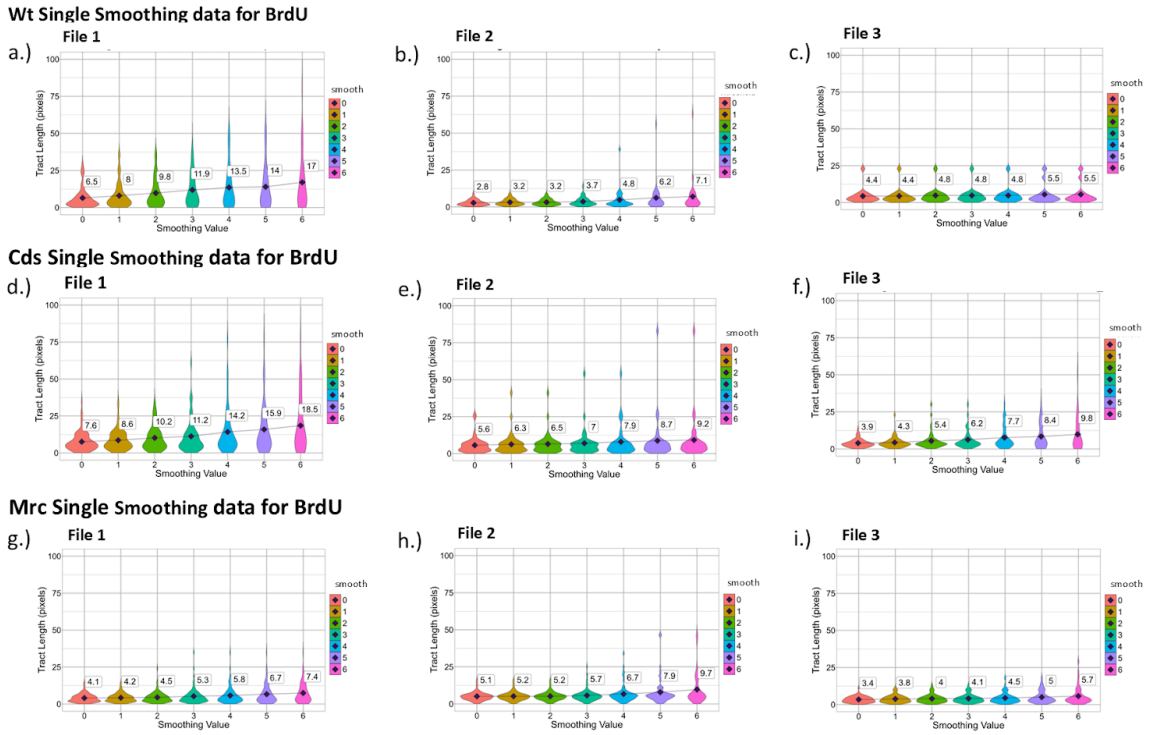

S5 Individual Replicates of BrdU Smoothing for Wt, cds1Δ and mrc1Δ. The individual BrdU lengths at the image slides of the three replicates of wt, cds1Δ, and mrc1Δ. (A-C) The violin plot shows different smoothing' effects on the three wt replicates. (D-F) The violin plot shows different smoothing' effects on the three cds1Δ replicates. (G-I) The violin plot shows different smoothing effects on the three mrc1Δ replicates.

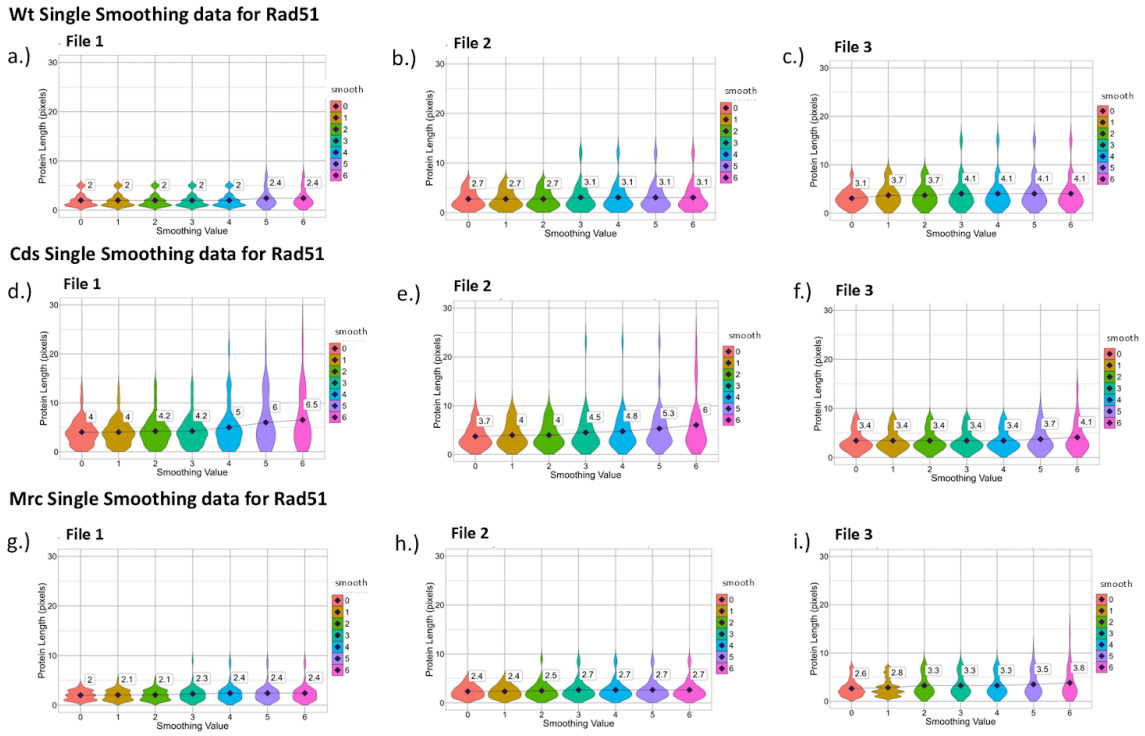

S6 Individual Replicates of Rad51 Smoothing for Wt, cds1Δ and mrc1Δ. The individual BrdU lengths at the image slides of the three replicates of wt, cds1Δ, and mrc1Δ. (A-C) The violin plot shows different smoothing' effects on the three wt replicates. (D-F) The violin plot shows different smoothing' effects on the three cds1Δ replicates. (G-I) The violin plot shows different smoothing effects on the three mrc1Δ replicates.

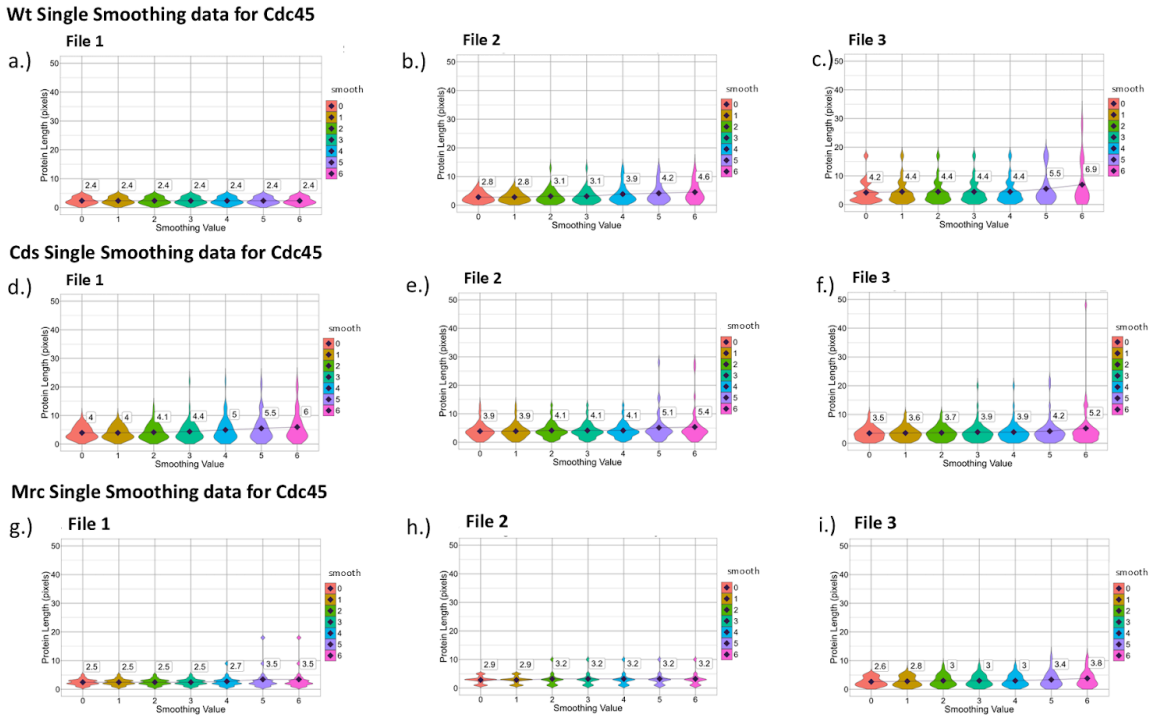

S7 Individual Replicates of Cdc45 Smoothing for Wt, cds1Δ and mrc1Δ. The individual BrdU lengths at the image slides of the three replicates of wt, cds1Δ, and mrc1Δ. (A-C) The violin plot shows different smoothing' effects on the three wt replicates. (D-F) The violin plot shows different smoothing' effects on the three cds1Δ replicates. (G-I) The violin plot shows different smoothing effects on the three mrc1Δ replicates.

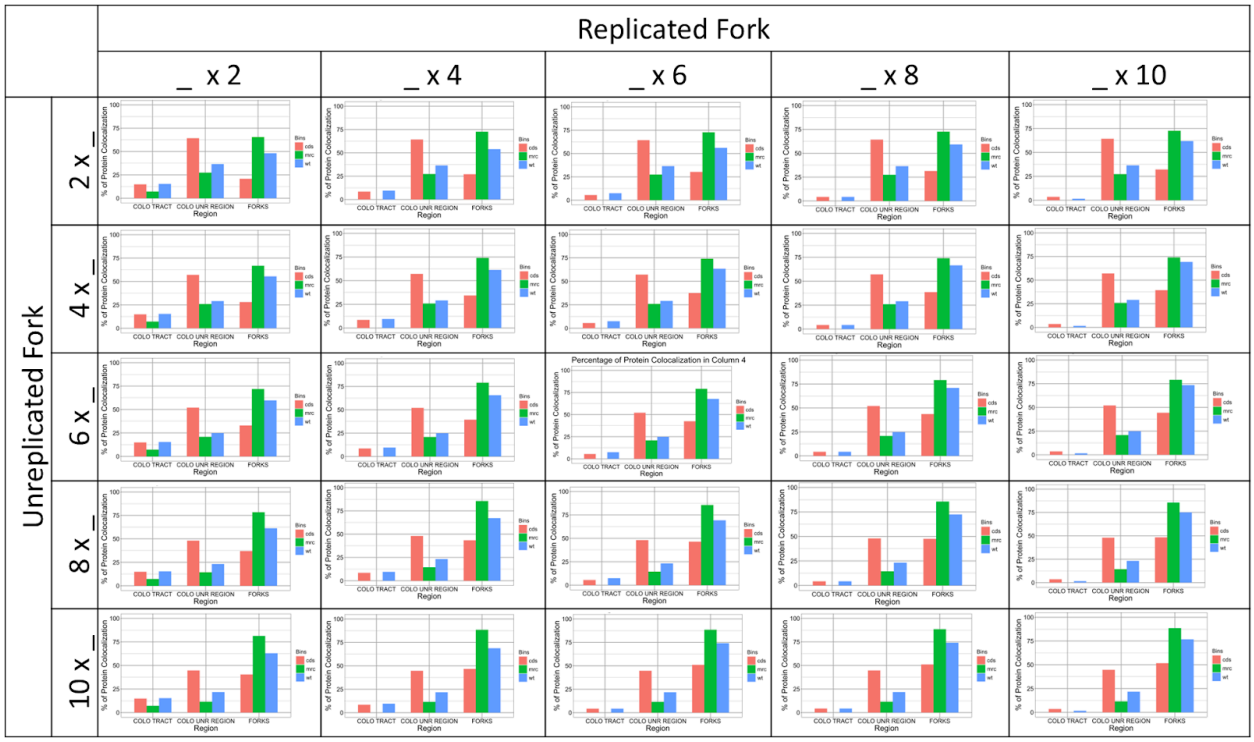

S8 Effects of Replication WIndow on Cdc45 colocalization. The multiple-grouped bar graph compares the effects of pixel designation of unreplicated and replicated forks on Cdc45-region colocalization. As the grid goes from up to down, the number of pixels in the unreplicated fork increases from 2- 10 in increments of 2. As the grid goes from left to right, the number of pixels in the replicated fork increases from 2- 10 in increments of 2.